Use of the Metabolic Tracer Carbon-11-Acetate for Evaluation of Regional Myocardial Perfusion

Sammy Y. Chan, Richard C. Brunken, Michael E. Phelps, and Heinrich R. Schelbert

Division of Nuclear Medicine and Biophysics, Department of Radiological Sciences, UCLA School of Medicine, and Laboratory of Nuclear Medicine, Laboratory of Biomedical and Environmental Sciences, University of California, Los Angeles, California

The high first-pass myocardial extraction fraction of carbon-11-acetate suggests that its initial uptake depends on blood flow. Accordingly, regional uptake of ^{11}C-acetate at 4 min was compared to regional perfusion determined with nitrogen-13-ammonia in 119 segments in 15 patients with stable coronary artery disease by two methods. A close correlation was observed between initial relative myocardial concentrations (segmental activity normalized to maximal activity) of both tracers (^{11}C-acetate = 0.88; ^{13}N-ammonia + 0.079; s.e.e. = 0.064, r = 0.94, $p < 0.001$). Furthermore, segmental net extractions (E·F), as calculated from the input function and segmental activities, of the two tracers correlated closely by $E \cdot F_{C-11} = 0.55E \cdot F_{N-13} + 0.080$ (s.e.e. = 0.045, r = 0.87, $p < 0.001$). These relationships indicate that initial regional myocardial uptake of ^{11}C-acetate reflects perfusion and that ^{11}C-acetate permits near simultaneous evaluation of regional oxidative metabolism and of regional myocardial perfusion.

J Nucl Med 1991: 32:665–672

Noninvasive evaluation of regional myocardial oxidative metabolism is possible with carbon-11-acetate (^{11}C-acetate) and dynamic positron emission tomography (PET). After i.v. injection, ^{11}C-acetate rapidly accumulates in the myocardium and clears in a biexponential fashion, mostly in the form of ^{11}C-labeled CO_2 (*1–3*). The slope of the rapid clearance curve component correlates closely with myocardial oxygen consumption (*3,4*). In open-chest dog experiments, myocardial first-pass extraction fractions of ^{11}C-acetate averaged 64.2% at control flows of 117.1 ml/min/1100 g (*4*). This high first-pass extraction fraction implies that initial uptake depends upon myocardial blood flow. It suggests that early images of ^{11}C-acetate in myocardium largely reflect the distribution of regional myocardial blood flow and may be useful for evaluating myocardial blood flow. Furthermore, the tracer rapidly disappears from blood while it is initially retained in myocardium. This short time period of relatively high myocardium-to-blood activity ratios allow the acquisition of high contrast images of the regional distribution of ^{11}C-acetate in the myocardium.

This study was performed in patients with chronic coronary artery disease and resting perfusion abnormalities to determine whether the initial uptake of ^{11}C-acetate in myocardium correlated with regional myocardial blood flow as delineated with nitrogen-13-ammonia (^{13}N-ammonia) as a tracer of blood flow. Such a correlation would allow the combined evaluation of regional myocardial blood flow and regional rates of oxidative metabolism with a single injection of ^{11}C-acetate.

METHODS

Patient Population

Fifteen patients with known coronary artery disease and stable angina were studied. They were referred by UCLA faculty and community cardiologists. None had unstable angina or had sustained an acute myocardial infarction within 14 days of the study. The demographic and clinical characteristics of the patients are listed in Table 1.

After explaining the rationale, investigative nature, and potential risks of the procedure, each patient signed an informed consent form approved by the University of California at Los Angeles Human Subject Protection Committee.

Study Protocol

PET. Nitrogen-13-ammonia and ^{11}C-acetate were produced at the UCLA Medical Cyclotron as previously described (*4,5*). Imaging was performed with a whole-body positron emission tomograph (Model 931/8; Siemens Gammasonics, Hoffman Estates, IL), which simultaneously acquires 15 transverse slices spaced 6.75 mm apart and covers a 11-cm axial field of view. The intrinsic in-plane resolution at the center of the field of view is 6.5 mm full width at half maximum. The performance characteristics of the tomograph have been described previously (*6*).

After positioning the patient in the tomograph, 20-min transmission images were acquired and used for subsequent correction for photon attenuation. An i.v. bolus of 15–20 mCi of ^{13}N-ammonia was then administered over 30 sec, while acquisition of serial cross-sectional emission images for 19–24 min was started. Forty-five to 60 min later, after physical decay of the ^{13}N activity to near undetectable levels, an i.v. bolus of 12 to 15 mCi of ^{11}C-acetate was administered over a 30-sec period, while ac-

Received Apr. 11, 1990; revision accepted Oct. 1, 1990.

For reprints contact: Sammy Y. Chan, MD, Division of Nuclear Medicine and Biophysics, UCLA School of Medicine, Los Angeles, CA 90024-1721.

TABLE 1
Demographic and Clinical Characteristics of Patients

Number	15
Sex (male/female)	10/5
Age mean (yr)	63.7 ± 8.2
range	50–77
History of MI	14
Coronary artery disease	
LAD only	1
LAD + CFx	3
LAD + PDA	4
LAD + CFx + PDA	7
Left Ventricular Failure	7
NYHA II	2
NYHA III	3
NYHA IV	2
LVEF mean (%)	35.0 ± 17.8
range	12–68
Sinus rhythm	15
Medications	
Nitrates	7
β-blockers	1
Ca-channel blockers	6
Anti-arrhythmics	3
Anti-coagulants	1
ACE inhibitors	4
Platelet inhibitors	5
Digoxin	4
Diuretics	6
Cholesterol lowering agents	4
Potassium supplements	6
Steroids	1*

* The single patient was on steroids for sarcoidosis that did not involve the heart.

quisition of serial PET images for 26–38 min commenced. Patient movement during and between both studies were minimized with the use of a velcro strap across the chest. The whole-body radiation dose to the patient was estimated to range from 0.015 to 0.020 rads for ^{13}N-ammonia (*7*) and 0.048 to 0.060 rads for ^{11}C-acetate (*8*), for a total whole-body dose of 0.063–0.080 rads per study.

Rapid serial PET imaging was performed to determine the arterial input function of tracer and the myocardial tissue response. The image acquisition sequences were as follows: for ^{13}N-ammonia, twelve frames of 10 sec each, followed by two frames of 60 sec each, and one frame of 900 sec. In five patients, a single frame of 1,200 sec duration was recorded instead of the last 900-sec frame. Thus, the total image acquisition time for ^{13}N-ammonia amounted to 19–24 min. For ^{11}C-acetate, six frames of 60 sec each were acquired initially, followed by ten frames of 120 sec each, amounting to a total acquisition time of 26 min. In five patients, six additional 120-sec frames were recorded for a total imaging time of 38 min.

All patients were studied post-prandially. Heart rate, blood pressure and electrocardiographic lead II were monitored at regular intervals throughout the study.

Image Analysis

The 15 simultaneously recorded cross-sectional images were reconstructed in a 128 pixel × 128 pixel matrix, which corresponded to an area of 20 × 20 cm in the field of view. A Shepp-Logan filter with a cutoff frequency of 0.15 cycles/sec was employed, resulting in an effective in-plane resolution of 11 mm FWHM. All images were corrected for photon attenuation. The contiguous cross-sectional images were normalized to each other. Spatial smoothing in the Z-axis direction was achieved by summing three adjacent planes resulting in an axial resolution of 15 mm (FWHM). The center plane was weighed by a factor of 2 and the two adjacent planes by a factor of 1. Planes 1 and 15 were not summed and were not used for analysis.

Five or six cross-sectional image planes encompassing the entire left ventricle from the apex to the base were utilized for image analysis. Using an operator-interactive, semi-automatic computer program described previously (*9*), the operator outlined the left ventricular myocardium on the cross-sectional images and assigned a small region of interest (ROI) to the left ventricular blood pool in the center of the ventricular cavity on the frame with the highest myocardial tissue-to-blood pool activity ratio. For ^{13}N-ammonia, this was the last of the serially acquired images. For ^{11}C-acetate studies, this was usually the fourth or fifth of the serially acquired frames. The region of the mitral valve plane was excluded from analysis. The ROI assigned to the left ventricular myocardium and the left ventricular blood pool were then copied to all serial images of a given plane. Proper alignment of these ROIs with left ventricular myocardium and blood pool on each of the sequential images was confirmed by visual inspection. If misalignments due to patient motion during image acquisition were noted, the outline was redefined manually by the operator for each image. Outlines of the left ventricular myocardium were then divided into 60 sectors of 6° each, originating from the posterior limb of the long-axis of the left ventricle and proceeding in a clockwise fashion. Average activity concentrations (counts/pixel/minute) were calculated for each sector, corrected for physical decay to the time of tracer injection, and used for generation of circumferential profiles of myocardial tissue activity in each plane.

Average ^{13}N and ^{11}C tissue concentrations were then calculated in eight anatomic segments of the left ventricle: anterobasilar, anterior, lateral, posterolateral and inferior walls, anterior and posterior septum, and the apex (Fig. 1). Assignment of the eight

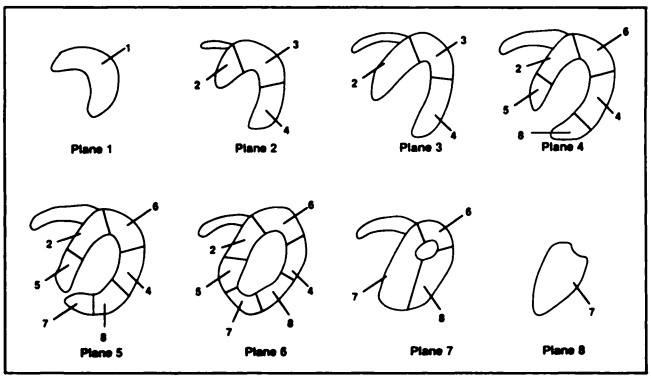

FIGURE 1. Assignment of anatomical segments. Reference standards for the assignment of segments are depicted. Each study plane is matched to one of the reference standards and the segments assigned according to the standard. (1) anterobasilar segment, (2) superior septum segment, (3) anterior wall segment, (4) lateral wall segment, (5) inferior septum segment, (6) apex segment, (7) inferior wall segment, and (8) posterolateral wall segment.

anatomical segments was identical for the ^{13}N-ammonia and the ^{11}C-acetate images in each patient. Total tracer tissue concentrations in each anatomical segment were calculated by multiplying average activity concentration (counts/pixel/minute) in a given sector by the number of pixels in that sector. The products were then summed for all 6° sectors located in a given anatomic segment and divided by the total number of pixels of all sectors in that segment. Thus, an average activity concentration was determined for each segment. The number of pixels per anatomic segment ranged from 147 to 556. Myocardial tissue time-activity curves of both ^{13}N-ammonia and ^{11}C-acetate were then generated for each anatomic segment. A time-activity curve for arterial blood was also generated by averaging the blood-pool ROIs of all planes with appropriate weighting for the number of pixels of the ROI in each plane.

Comparison Between Regional ^{13}N and ^{11}C Activity Concentrations

Two approaches were used: The first approach examined the relative distributions of tracer activity concentrations and the second compared myocardial net extractions of both tracers.

Relative Tracer Concentrations. The highest segmental activity for each patient study was defined as 1.0. Activity concentrations in the remaining seven myocardial segments were then expressed as a fraction of the maximum activity. This normalization of tissue activity concentrations to the peak activity corrects for the differences in activity doses of radiotracers administered to individual patients. The last of the serial ^{13}N-ammonia images was analyzed because blood-pool activity at that time had reached a minimum, while myocardial tissue activity remained high. For the ^{11}C-acetate study, images recorded 4 min after tracer injection were analyzed, as ^{11}C activity concentrations were highest in myocardium and relatively low in the left ventricular blood pool.

Myocardial Net Extraction of Tracer. Regional myocardial activity concentrations of tracer are a function of the first-pass extraction fraction E, regional myocardial blood flow F, and the arterial input function. The myocardial activity concentration Q(T) is described by:

$$Q(T) = E \cdot F \cdot \int_0^T C_a(t)dt, \qquad \text{Eq. 1}$$

where Q(T) is the regional activity concentration at time T after tracer injection and $C_a(t)$ is the arterial tracer activity concentration at time T as determined from serial cross-sectional images. The net extraction (E·F) was determined by rearranging Equation 1 to:

$$E \cdot F = Q(T) / \int_0^T Ca(t)dt \qquad \text{Eq. 2}$$

or by dividing the regional myocardial tracer tissue activity at time T by the integral of the arterial input function to time T. For ^{13}N-ammonia, myocardial tissue activity was determined on the last serial image, while the arterial input function was integrated only over the first 2 min. This method of calculation was undertaken because previous studies have shown that the myocardial uptake of ^{13}N-ammonia is virtually complete at 2 min and myocardial ^{13}N tissue activity concentrations change little thereafter (*10*). Furthermore, most of the ^{13}N activity in arterial blood after 2 min is bound to urea and amino acids rather than ammonia (*11*). Integration of the arterial tracer activity concentrations beyond this time would therefore overestimate the true arterial input function of ^{13}N-ammonia. For ^{11}C-acetate, the myocardial net extraction was calculated from the myocardial tissue activity on the image acquired during the fourth minute after tracer injection and arterial input function integrated over the first 4 min. Because ^{11}C-acetate may already have cleared from myocardium at that time, net extractions calculated in this manner provide only an estimate of true net extraction of the tracer by myocardium.

Statistical Analysis

Relative tracer concentrations and myocardial net extractions were compared by linear regression analysis. Mean values, slopes, and y-intercepts are given with standard errors. Student's t-test was used to determine the significance of the correlation coefficient. A probability value of <0.05 was considered significant.

RESULTS

Hemodynamic Data

All patients remained hemodynamically stable throughout the ^{13}N-ammonia and ^{11}C-acetate study. There were no significant changes observed in the heart rate (72.6 ± 18.5 versus 72.6 ± 18.4 bpm, p = ns) or systolic blood pressure (115.8 ± 16.5 versus 115.8 ± 16.1 mmHg, p = ns) between the ^{13}N-ammonia and ^{11}C-acetate studies. Therefore, cardiac work, as expressed by similar heart rates and systolic blood pressure was constant during the ^{13}N-ammonia and the ^{11}C-acetate studies, implying that myocardial blood flow did not change between the two studies.

Image Quality

Total counts of 30 million were routinely achieved for the last image of ^{13}N-ammonia study and of 2 million for the fourth dynamic image of the ^{11}C-acetate study. Average count rates in normal myocardial segments were approximately 21 counts/pixel/minute for both tracers. Given the different acquisition times, this resulted in total counts of 63,000–231,000 per anatomic segment for the ^{13}N-ammonia and 3,200–11,600 counts/segment for ^{11}C-acetate. Myocardial-to-blood pool ratios were usually 5 to 1 for ^{13}N-ammonia images and 4 to 1 for the ^{11}C-acetate images.

Myocardial Regional Tissue Activity Concentrations

Tissue time-activity curves for ^{13}N-ammonia are shown in Figure 2 and for ^{11}C-acetate in Figure 3. As shown in Figure 2, ^{13}N-ammonia rapidly accumulates in myocardium and rapidly clears from arterial blood. The early peak on the myocardial time activity curve for ^{13}N-ammonia is caused by physical spillover of activity from blood into myocardium, as well as by ^{13}N activity in the vascular compartment of the myocardium. Net extractions of ^{13}N-ammonia were calculated from the integral of the arterial input function to 2 min and from the myocardial ^{13}N concentrations on the last of the serial images. As noted in Figure 3, myocardial ^{11}C activity concentrations after i.v. ^{11}C-acetate injection rapidly reach a plateau of about 2–3 min duration after which ^{11}C activity clears biexponentially from myocardium. Images recorded at 4 min, during the time of myocardial peak activity, were used to

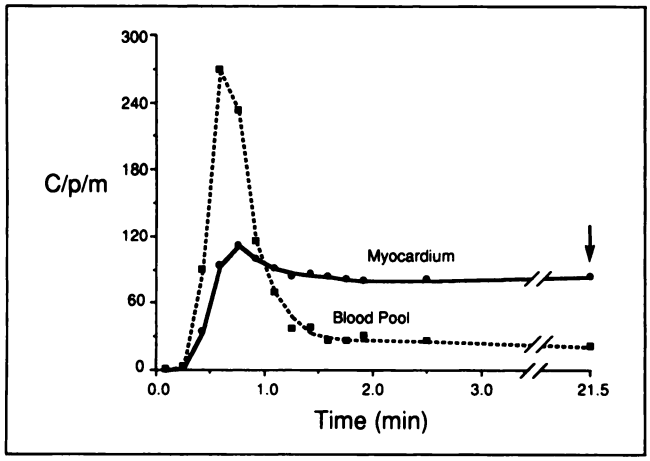

FIGURE 2. Time-activity curve for ^{13}N-ammonia. The myocardial tissue and blood-pool time-activity curve for ^{13}N-ammonia. The arrow indicates the dynamic time frame used in the calculations of relative tissue concentrations and net extractions. The early peak in myocardium is due to spillover from blood pool. Once tissue uptake of the tracer is completed, tracer concentration changes minimally for the remainder of the study.

determine the relative myocardial ^{11}C concentrations and for calculation of the regional myocardial net extractions.

Three contiguous ^{13}N-ammonia and ^{11}C-acetate myocardial images in one of the patients with a prior anterior myocardial infarction are shown in Figure 4A. The ^{13}N-ammonia image was acquired from 5 to 19 min and the ^{11}C-acetate image at 4 min after tracer injection. Both image sets demonstrate similar distributions of ^{13}N and ^{11}C activity throughout the left ventricular myocardium. Consistent with the patient's prior myocardial infarction,

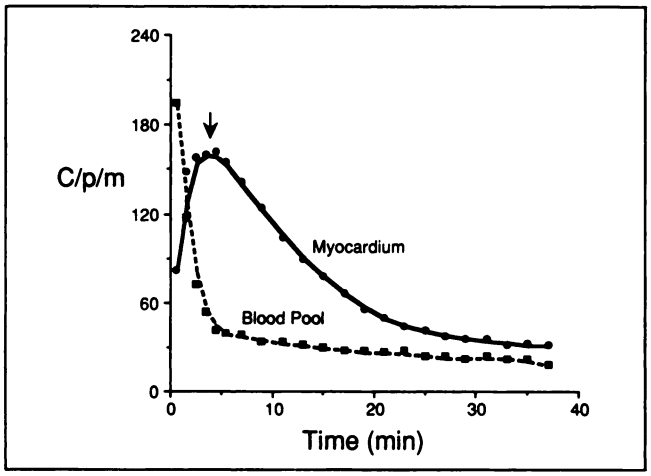

FIGURE 3. Time-activity curve and the myocardial tissue and blood-pool time-activity curve for ^{11}C-acetate. The arrow indicated the dynamic time frame used in the calculations of relative tissue concentrations and net extractions. Following injection, tissue tracer concentration increases until approximately the fourth minute before declining. At that time blood-pool tracer concentration has decreased almost to baseline levels. Thus, a time window exists whereby external imaging can accurately detect tissue tracer concentration.

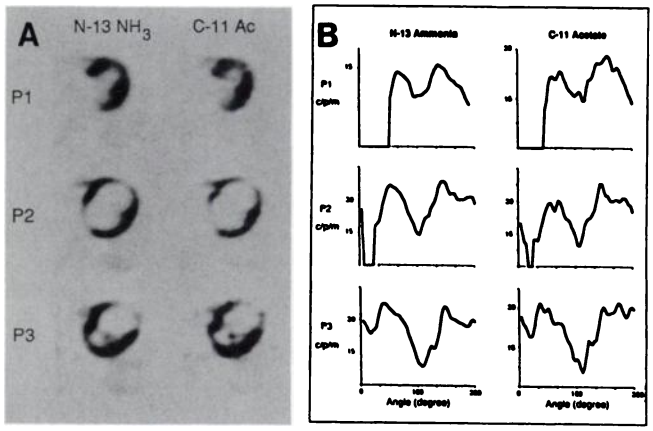

FIGURE 4. (A) Comparison between three contiguous ^{13}N-ammonia and ^{11}C-acetate images. Three planes of both ^{13}N-ammonia and ^{11}C-acetate studies are depicted. The left panel represents the ^{13}N-ammonia study and the right panel the ^{11}C-acetate study. The images are oriented so that the anterior wall is superior, the septum is towards the left side, and the free wall is on the right side. This patient had sustained an anterior infarction previously. This is evidenced on the images by the decreased tissue concentration of both ^{13}N-ammonia and ^{11}C-acetate in the anterior wall. The tissue concentrations of the ^{11}C-acetate study resemble those of ^{13}N-ammonia closely. (B) Corresponding circumferential profiles. The circumferential profiles of the ^{13}N-ammonia images are outlined on the left and those of the ^{11}C-acetate study on the right. There are some minor variations but overall the paired profiles are similar to one another.

tracer concentrations are markedly reduced in the anterior wall. Circumferential profiles for these images depict the similar activity concentrations for both tracers in the same patient (Fig. 4B).

Relative Activity Distribution

Relative ^{13}N and ^{11}C tracer activity concentrations were similar in each of the eight myocardial segments as exemplified in one patient in Table 2 and Figure 5A. In all 15 patients, 119 paired anatomic segments of both ^{13}N-ammonia and ^{11}C-acetate studies were available for analysis. One segment was excluded from analysis because it was not visualized on the ^{11}C-acetate study due to patient motion between the ^{13}N-ammonia and the ^{11}C-acetate study. When relative activity concentrations of ^{13}N-ammonia and ^{11}C-acetate were compared separately for each of the eight anatomic segments, the slopes and y-intercepts of the regression lines were similar for all segments as determined by analysis of variance (Table 3, for slope, $F = 0.05$, p = ns; for y-intercept, $F = 0.04$, p = ns). Thus, the relationship between relative ^{13}N and ^{11}C activity concentrations was similar in each of the eight anatomic segments of the left ventricle. All data pairs were therefore grouped together and analyzed by linear regression analysis. The lowest relative activity in any of the segments was 0.31 for ^{13}N and 0.35 for ^{11}C activity. As depicted in Figure 6, the relative segmental ^{13}N-ammonia tissue activity concentrations correlated well with relative segmental ^{11}C-acetate concentrations ($y = 0.88x + 0.079$, s.e.e. = 0.064,

TABLE 2
Sizes, Tissue Activities, Relative Concentrations, and Net Extractions of Each Anatomic Segment in a Patient

Myocardial Segment	Segment size (pixels)	Tissue activity (counts/pixel/min)		Relative concentration (%)		Net extraction	
		^{13}N	^{11}C	^{13}N	^{11}C	^{13}N	^{11}C
Ant-bas	163	18.45	17.40	98.6	92.9	0.44	0.38
Sup. sep	514	18.75	18.60	100.0	100.0	0.44	0.41
Ant. wall	422	11.25	12.45	60.2	66.7	0.27	0.27
Lat. wall	556	17.10	16.80	91.3	90.2	0.40	0.37
Inf. sep	273	9.45	10.95	50.5	59.1	0.22	0.24
Apex	365	6.45	8.25	34.9	44.0	0.15	0.18
Inf. wall	147	8.40	7.80	45.2	42.0	0.20	0.17
Postlat. wall	327	11.10	12.90	59.4	69.3	0.26	0.28

Abbreviations: Ant-bas = anterobasilar segment; Sup. sep = superior septum segment; Ant. wall = anterior wall segment; Lat. wall = lateral wall segment; Inf. sep = inferior septum segment; Apex = apex segment; Inf. wall = inferior wall segment; and Postlat. wall = posterolateral wall segment.

FIGURE 5. (A) Relative concentrations in a patient example. The relationship between the relative concentrations of ^{13}N-ammonia and ^{11}C-acetate in one patient is depicted. As noted in Table 1, the tissue activity of the superior septum is highest in this patient and is designated as 100%. The activity of the remaining segments are then calculated relative to the superior septum. The data fit well to a linear function. (B) Segmental net extractions in a patient example. The relationship between the segmental net extractions of ^{13}N-ammonia and ^{11}C-acetate in one patient is depicted. The data fit well to a linear function but have a slope less than 1 and a positive y-intercept.

r = 0.94, $p < .001$, 95% confidence interval for slope = 0.82 – 0.94; for y-intercept = 0.033 – 0.125). The regression line has a slope of less than unity and a positive y-intercept.

Myocardial Tracer Net Extractions

Comparison of segmental myocardial net extractions of ^{13}N-ammonia and ^{11}C-acetate revealed close agreement in individual patients (Figure 5B). Separate comparisons of ^{13}N and ^{11}C net extractions for each of the eight anatomic segments revealed no systematic intersegmental differences (Table 3). Therefore, all data pairs for segmental myocardial net extractions were grouped together and submitted to linear regression analysis. Segmental tracer net extractions ranged from 0.13 to 0.78 for ^{13}N-ammonia and from 0.12 to 0.52 for ^{11}C-acetate. As shown in Figure 7, segmental net extractions of ^{13}N-ammonia correlated well with ^{11}C-acetate ($y = 0.55x + 0.08$, s.e.e. = 0.045, r = 0.87, $p < 0.001$, 95% confidence interval for slope = 0.49 – 0.61; for y-intercept = 0.051 - 0.103.)

DISCUSSION

This study demonstrates a close correlation of ^{11}C-acetate to segmental myocardial ^{13}N-ammonia uptake and,

TABLE 3
Parameters of Regression Lines of Relative Concentrations and Net Extractions for Each Anatomic Segment

	Relative concentrations			Net Extraction		
Segment	Slope	Intercept	Corr. Coeff.	Slope	Intercept	Corr. Coeff.
Ant bas	0.92 ± .08	0.00 ± .07	0.95	0.54 ± .07	0.07 ± .04	0.89
Sup. sep	0.97 ± .16	0.00 ± .15	0.86	0.38 ± .12	0.17 ± .06	0.66
Ant. wall	0.80 ± .08	0.11 ± .05	0.95	0.51 ± .08	0.08 ± .03	0.87
Lat. wall	0.97 ± .08	0.05 ± .07	0.96	0.61 ± .09	0.07 ± .04	0.89
Inf. sep	0.75 ± .09	0.19 ± .08	0.91	0.42 ± .08	0.13 ± .04	0.82
Apex	0.74 ± .06	0.16 ± .03	0.96	0.46 ± .07	0.09 ± .02	0.89
Inf. wall	0.90 ± .08	0.07 ± .07	0.95	0.55 ± .08	0.08 ± .04	0.88
Postlat. wall	0.94 ± .15	0.06 ± .13	0.87	0.59 ± .12	0.08 ± .06	0.80
ANOVA for relative concentration				ANOVA for net extraction		
slope:F-ratio = 0.05, p = ns				slope:F-ratio = 0.02, p = ns		
y-intercept:F-ratio = 0.04, p = ns				y-intercept:F-ratio = 0.05, p = NS		

Mean values are given with standard errors. The slopes and y-intercepts of the regression lines for the relative concentration of ^{13}N-ammonia against ^{11}C-acetate and for the net extraction of ^{13}N-ammonia against ^{11}C-acetate for the eight anatomic segments are not significantly different from one another.
Abbreviations: See Table 2.

thus, perfusion in patients with stable coronary artery disease at rest. This close correlation between both tracer tissue concentrations, readily apparent on visual inspection of the images, was confirmed by quantitative image analysis. The relative concentrations as well as segmental tracer net extractions correlated closely for both tracers. The results indicate that segmental myocardial blood flow can be evaluated from the initial ^{11}C-acetate uptake images.

Despite these close correlations, the regression lines for both the relative activity concentrations and the net extractions, have a slope of less than one and a positive y-intercept. Several factors may account for these findings. First, ^{13}N-ammonia is metabolically trapped in myocardium. Tissue ^{13}N concentrations are relatively constant after 2 min. In contrast, ^{11}C-acetate rapidly accumulates in myocardium but subsequently clears from it. Tissue clearance half-times during the early part of the dynamic ^{11}C-acetate study are on the order of 10 min in normal myocardium (*12*). Therefore, when ^{11}C activity concentra-

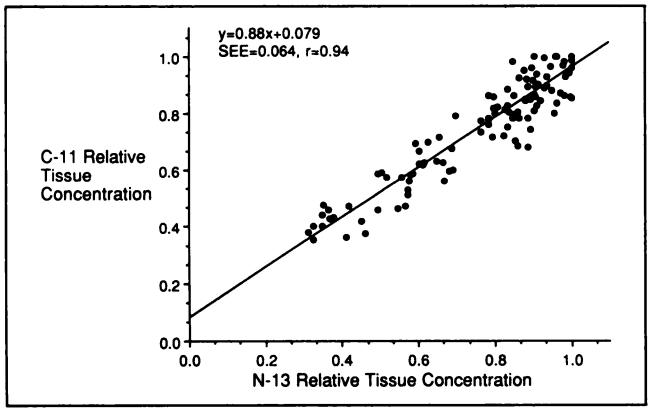

FIGURE 6. Comparison of relative segmental activity concentrations of ^{13}N-ammonia and ^{11}C-acetate. The relationship between segment tracer activity concentrations of ^{13}N-ammonia and ^{11}C-acetate in 119 segments from 15 patients. The activity concentration in each segment is normalized to the peak segmental activity of that tracer in each study. The data are fitted to a linear function. The resultant regression line has a slope of less than 1 and a y-intercept greater than 0.

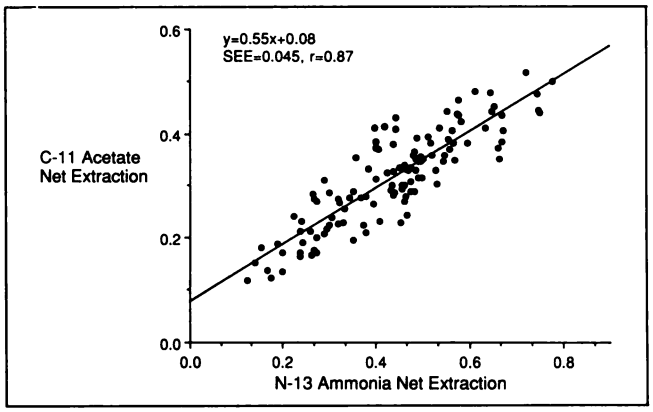

FIGURE 7. Comparison of segmental net extractions for ^{13}N-ammonia for ^{11}C-acetate. The relationship between the segmental net extractions for ^{13}N-ammonia and ^{11}C-acetate in 119 segments from 15 patients. Net extractions were calculated by dividing the segmental tissue tracer concentration by the arterial input. The data are then fitted to a linear function. The slope of the regression line is less than 1 and the y-intercept is positive.

tions are measured at 4 min after injection, a fraction of the ^{11}C activity was likely to have already been released from myocardium and tissue concentrations at the time probably underestimated the true net extraction of tracer.

Second, ratios of tracer uptake to clearance rates are likely to vary within myocardium because of regional differences in blood flow and, consequently, oxidative metabolism. Carbon-11-acetate concentrations decline less rapidly in hypoperfused myocardium than in normal tissue because of the higher rates of oxidative metabolism in normal myocardium. Consequently, relative to blood flow, regional ^{11}C-acetate concentrations at 4 min are likely to be lower in normally perfused than in hypoperfused myocardial regions.

Third, differences in first-pass extraction fractions and their dependency on blood flow are another possible explanation. Schelbert et al. (*13*) described the relation between myocardial first-pass extraction fractions (E) of ^{13}N-ammonia and myocardial blood flow (F) by $E = 1 - 0.609e^{-1.25/F}$. For ^{11}C-acetate, Armbrecht et al. (*4*) found the relationship to be $E = 1 - 0.58e^{-0.44/F}$. Thus, for low-to-normal blood flows, the first-pass extraction fraction of ^{11}C-acetate is less than that of ^{13}N-ammonia. Furthermore, the net extractions of both tracers change nonlinearly as blood flow increases; at physiologic blood flow ranges, the net extraction of ^{11}C-acetate increases less than that of ^{13}N-ammonia. This divergence of tracer net extractions in response to increases in blood flow results in a non-linear relationship between the net extractions for both tracers. Thus linear least-squares fitting of the net extractions as performed in this study results in a slope of less than unity and has positive y-intercept.

The same factors also explain the observations on the relative distributions of both tracers in myocardium. As described in Equation 1, the segmental tracer tissue concentration in myocardium is the product of the segmental first-pass extraction fraction, regional blood flow, and the integral of the arterial tracer input function. In any given patient, the arterial input function is identical for all segments. Thus, relative tissue concentration of any segment depends on the ratio of the E·F product in that segment to the E·F product in the segment with the highest tracer concentration. At low blood flows, the products for both tracers differ only slightly. At peak flows, however, the product for ^{11}C-acetate is much less than for ^{13}N-ammonia. The combination of only a small difference between the products at low flows, but a progressively larger difference at higher flows results in a non-linear relationship between relative segmental tracer activities and its consequent effect on the slope of a linear regression line.

Although count rates were similar for both the ^{13}N-ammonia and the ^{11}C-acetate studies, early clearance of ^{11}C activity from myocardium limited the image acquisition times for ^{11}C-acetate to only 1 min. Total counts per myocardial segment were therefore much lower. This reduction in count statistics for ^{11}C-acetate may limit accurate evaluation of blood flow in severely hypoperfused myocardial regions.

No gating was used in this study to acquire the early part of arterial input function. Since there was no change in cardiac work between the two studies, cardiac wall motion should not differ between the two studies. Therefore, the effects of cardiac wall motion on tissue tracer concentration is similar for both tracers and should not affect direct comparisons between them. Similarly, partial volume effects should equally affect both tissue tracer concentrations. Tissue tracer concentrations for both ^{13}N and ^{11}C were measured at a time when blood-pool concentrations of the tracers had decreased to minimal levels, so spillover of activity from the blood pool is negligible.

We employed ^{13}N-ammonia in this study as a tracer of regional myocardial blood flow against which the initial uptake of ^{11}C-acetate was tested. The validity of ^{13}N-ammonia for the evaluation as well as for quantification of regional myocardial blood flow has been previously demonstrated in animal experimental studies and in clinical investigations (*5,13–15*). Similarly, net extractions of ^{13}N-ammonia, as determined in this study, were found to be a useful quantitative index of regional myocardial blood flow (*10,16*). Integration of the arterial input function for ^{13}N-ammonia for only the first 2 min after injection avoided contamination of metabolites as well as spillover of activity from myocardium into the blood pool (*11,17*), which may result in an overestimation of the true tracer input function. For ^{11}C-acetate, contamination of the arterial input function by labeled metabolites has not been explored systematically. Preliminary findings in our laboratory suggest that the fraction of the primary labeled metabolite, $^{11}C\ CO_2$, amounts to less than 7% of the total arterial activity concentration at 4 min after tracer injection.

The close correlation between myocardial net extractions of ^{11}C-acetate and ^{13}N-ammonia suggests the possibility of deriving quantitative information on regional myocardial blood flow from the dynamically acquired ^{11}C-acetate PET images. This assumes that the first pass extraction fraction of ^{11}C-acetate is not altered by changes in plasma substrate levels or by changes in myocardial metabolism. This assumption, however, remains to be tested.

The severity of coronary disease in our patients ranged from single- to three-vessel disease, with a wide spectrum of left ventricular functions. Our findings should therefore be applicable to patients with stable coronary artery disease. Because studies were performed only in the resting state, it is not clear whether similar results would be noted at hyperemic flow ranges. Further studies are needed to determine whether our findings also apply to acute ischemic states, following myocardial reperfusion, as well as in patients with intrinsic myocardial disease.

Evaluation of both myocardial perfusion and oxidative metabolism with a single tracer is advantageous. Use of a

single isotope to examine two physiologic processes would reduce the radiation burden to the patient. In our case, if a single ^{11}C-acetate study had replaced the combination ^{13}N-ammonia and ^{11}C-acetate study, the radiation exposure would be decreased by approximately 25%, and the time required to complete the study would be shortened from 120 to 60 min with an attendant increase in patient comfort.

In conclusion, we found that there is a close relationship between the early myocardial tissue activity of ^{11}C-acetate and the equilibrium tissue activity of ^{13}N-ammonia at rest. This relationship was apparent by visual inspection of the ^{13}N-ammonia equilibrium image and an early ^{11}C-acetate image. In addition, the early net extraction of ^{11}C-acetate also correlated with the net extraction of ^{13}N-ammonia. These results imply that the early uptake and distribution of ^{11}C-acetate reflects myocardial blood flow and therefore may be useful in the demonstration of myocardial perfusion patterns in patients with chronic coronary artery disease. They also suggest that quantitation of myocardial blood flow may be feasible with ^{11}C-acetate.

ACKNOWLEDGMENTS

The authors thank Ron Sumida, Lawrence Pang, Francine Aguilar, Gloria Stocks, Anne Irwin, Judy Edwards, and the staff of the Medical Cyclotron at UCLA for technical assistance. We thank Kerry Engber for secretarial assistance and Lee Griswold and Wendy Wilson for preparing the illustrations.

Operated for the U.S. Department of Energy by the University of California under Contract #DE-FC03-87ER60615. This work was supported in part by the Director of the Office of Energy Research, Office of Health and Environmental Research, Washington, DC, by research grants #HL 29845 and #HL 33177, National Institutes of Health, Bethesda, MD and by an Investigative Group Award by the Greater Los Angeles Affiliate of the American Heart Association, Los Angeles, CA.

Dr. Brunken is the recipient of a Clinical Investigator Award (#HL 02022-02) from the National Institutes of Health, Bethesda, MD.

REFERENCES

1. Brown M, Marshall DR, Burton BS, Sobel BE, Bergmann SR. Delineation of myocardial oxygen utilization with carbon-11-labeled acetate. *Circulation* 1987;76:687–696.
2. Buxton DB, Schwaiger M, Nguyen A, Phelps ME, Schelbert HR. Radiolabeled acetate as a tracer of myocardial tricarboxylic acid cycle flux. *Circ Res* 1988;63:628–634.
3. Buxton DB, Nienaber CA, Luxen A, et al. Noninvasive quantitation of regional myocardial oxygen consumption in vivo with [1-^{11}C] acetate and dynamic positron emission tomography. *Circulation* 1989;79:134–142.
4. Armbrecht JJ, Buxton DB, Schelbert HR. Validation of [1-^{11}C] acetate as a tracer for noninvasive assessment of oxidative metabolism with positron emission tomography in normal, ischemic, post-ischemic, and hyperemic canine myocardium. *Circulation* 1990;81:1594–1605.
5. Schelbert HR, Phelps ME, Hoffman EJ, Huang SC, Selin CE, Kuhl DE. Regional myocardial perfusion assessed with N-13-labeled ammonia and positron emission computerized axial tomography. *Am J Cardiol* 1979;43:209–218.
6. Spinks TJ, Jones T, Gilardi MC, Heather JD. Physical performance of the latest generation of commercial positron scanner. *Trans Nucl Sci* 1988;35:721–725.
7. Lockwood AH. Absorbed doses of radiation after an intravenous injection of N-13-ammonia. *J Nucl Med* 1980;21:276–278.
8. Snyder W, Ford M, Warner G, Watson S. "S," absorbed dose per unit cumulated activity for selected radionuclides and organs. MIRD pamphlet no. 5. *J Nucl Med* 1975;11:16–17.
9. Ratib O, Bidaut L, Nienaber C, Schelbert HR, Phelps ME. Semiautomatic software for quantitative analysis of cardiac positron tomography studies. *SPIE* 1988;914:412–419.
10. Shah A, Schelbert HR, Schwaiger M, et al. Measurement of regional myocardial blood flow with N-13-ammonia with positron emission tomography in intact dogs. *J Am Coll Cardiol* 1985;5:92–100.
11. Rosenspire KC, Schwaiger M, Mangner TJ, Hutchins GD, Sutorik A, Kuhl DE. Metabolic fate of [^{13}N]ammonia in human and canine blood. *J Nucl Med* 1990;31:163–167.
12. Armbrecht JJ, Buxton DB, Brunken RC, Phelps ME, Schelbert HR. Regional myocardial oxygen consumption determined noninvasively in humans with [1-^{11}C]acetate and dynamic positron tomography. *Circulation* 1989;80:863–872.
13. Schelbert HR, Phelps ME, Huang SC, et al. N-13-ammonia as an indicator of myocardial blood flow. *Circulation* 1981;63:1259–1272.
14. Krivokapich J, Smith GT, Huang SC, Ratib O, Phelps ME, Schelbert HR. Nitrogen-13-ammonia myocardial imaging at rest and with exercise in normal volunteers: quantification of absolute myocardial perfusion with dynamic positron emission tomography. *Circulation* 1989;80:1328–1337.
15. Schelbert HR, Wisenberg G, Phelps ME, et al. Noninvasive assessment of coronary stenoses by myocardial imaging during pharmacologic coronary vasodilation. VI. Detection of coronary artery disease in human beings with intravenous N-13-ammonia and positron computed tomography. *Am J Cardiol* 1982;49:1197–1207.
16. Nienaber C, Ratib O, Weinberg I, et al. noninvasive quantification of regional myocardial blood flow with N-13-ammonia and dynamic positron tomography. *J Am Coll Cardiol* 1988:10A.
17. Weinberg IN, Huang SC, Hoffman EJ, et al. Validation of PET-acquired functions for cardiac studies. *J Nucl Med* 1988;29:241–247.